International Journal For Advanced Research In Science & Technology
A peer reviewed international journal www.ijarst.in
ISSN: 2457-0362

Taguchi based Grey Relational Analysis and Analysis of Variance of Submerged Friction Stir Welding for Optimization of Mechanical and Metallurgical Properties of AA5083 Weld Bead

SK HUSSIAN BASHA 1, R VISWANATHAN 2,
ASSISTANT PROFESSOR 1 PROFESSOR 2,,
Mail ID; hussainn.shaik@gmail.com, Mail ID:mechhod@pallaviengineeringcollege.ac.in,
Dept.: Mechanical
Pallavi Engineering College,
Kuntloor(V),Hayathnagar(M),Hyderabad,R.R.Dist.-501505.

ABSTRACT

Friction stir welding has the potential to improve weld zone mechanical quality (FSW). The purpose of this work is to establish what combinations of FSW process parameters between two AA5083 plates will result in the most robust welds. Tool rotational speed (TRS) and tool transverse speed (TTS) are crucial characteristics in the FSW process, and submerged and normal FSW are two of the most prevalent weld process situations. This research makes use of an orthogonal array of experiments, or L18 Taguchi design. The Grey Relational Analysis (GRA) is utilized in combination with other parameters like as tensile strength, microhardness, and surface roughness to calculate the grey relation grade. The process's most crucial components have been identified, and ANOVA is utilized to maintain their manageability. Our FSW joints are the toughest on the market because we use optimal production parameters. This peculiarity becomes obvious while working with a submerged FSW, a fast-rotating tool, and a slow traversing speed (TTS).

Keywords:

Submerged friction stirs welding; mechanical properties; Taguchi method; Grey relational analysis (FSW).

INTRODUCTION

Welding of nonstandard materials with suitable mechanical qualities and surface quality is required for joint production. There is a connecting method called fusion-seam welding (FSW) that doesn't involve melting the materials being joined. Connecting two butted sides of the same or different metals using a single-use tool is how this method works. Generally speaking, combination welding of aluminium alloys is not recommended due to hot cracking and compound isolation issues. While keeping a constant heat output, submerged FSWs (SFSWs) may control the temperature in the HAZ surrounding the weld joint (Sabari et al., 2016). To a larger degree than if the material were moved from the front to the back of the tool at a lower rate of rotation, the mechanical strength of the weld joints is impacted by the tool's rotational speed (Fuji et al., 2006 and Suresh et al., 2011). Reduced-ultimate-temperature, lower-grain-growth weld joints are employed in the performance and analysis of Submerged FSW investigations. Over time, improved grain structure and superior mechanical characteristics led to increased ductility (Darras et al., 2013; Hofmann et al., 2005; Shanaaz et al., 2018; and Pedapati et al., 2017). At very high temperatures, the FSW undergoes plastic deformation, almost finishing the phase with polished grains (Jata et al., 2000; Liu et al., 1997).

Strong, high-output welds may be achieved by modifying a number of distinct process factors. Lowest hardness was observed at the HAZ on the sidewalls of AA5083 (Koilraj et al.,2012).

EXPERIMENTATION

In this experiment, we use an AA5083 plate that is 250 mm in length, 6 mm in thickness, and 60 mm in width. Table 1 lists the chemical properties, whereas Table 2 lists the mechanical ones. Figures 1 (a) and (b) demonstrate the experimental setup for butt welding AA5083 plate samples using the FSW method

The chemical makeup of AA5083 aluminum alloys is listed in Table 1 below.

Element	Si	Cu	Fe	Mg	Mn	Zn	Cr	Ti	Al
Wt.%	0.4	0.1	0.4	4.0-4.9	0.4-0.1	0.15	0.25	0.05-0.25	bal

Table 2. AA5083 mechanical properties.

Property	Value
Proof Stress	125 Min MPa
Ultimate Tensile Strength	275 - 350 MPa
Vickers Hardness	81 HV

Using an FSW-3TN-NC equipment, the FSW procedure is carried out routinely in air and under saltwater. Figures 1a and b depict the transformation of the conventional FSW machine

International Journal For Advanced Research In Science & Technology
A peer reviewed international journal www.ijarst.in
ISSN: 2457-0362

setup into the submerged FSW configuration. The H13 tool steel cylinder taper tool has a 5.8 mm long pin, a bigger diameter of 6, and a smaller diameter of 3 mm. The shoulder diameter is 18 mm.

a) A typical experimental configuration for FSW is shown in Figure 1. Setup for conducting experiments with submerged FSW (b).

As many transverse rates of speed (TRSs) as possible are used to weld the alloy plates. It tilted at an angle of 1 degree from the horizontal surface of the workbench, and the welding tool turned anticlockwise. Ethanol is used to remove the oily coating and oxide before welding. Kakinada's shoreline collects seawater in the submerged state. For the Submerged FSW experiment, seawater is employed. Image 2 shows the welded plates. A water jet cutting machine is used to cut the welded plates to the specified vertical length along the welding axis.

Figure 2. Welded samples were either submerged or performed under normal FSW conditions. The tensile specimens are constructed according to the ASTM D-358 parameters provided in Fig. 3 and evaluated using a computerized UTM (INSTRON-8801) as shown in Fig. 4. Microhardness samples are typically produced in a parallel fashion to the weld seam. Using an MH-5D digital hardness analyzer, we apply a force of 300 grams for a duration of 10 seconds to measure the Vickers microhardness of the weld zone. Scanning electron microscopy (SEM) equipped with an energy-dispersive X-ray spectrometer is used to examine the microstructures of the fracture surface of the FSW joint fracture tensile test samples (EDS). Joint is rinsed with etching solution (2ml HF+5ml HNO3+95mlpurified water) for the Al alloy many times using a cotton ball after the sample has been machined and polished until a discernible etching is produced. Finally, after a brief wash in water, the samples are disinfected with ethanol.

Figure 3. Materials with a high degree of tension. Diagram of the UTM System (INSTRON-8801).

An Examination of the Taguchi-Grey Relationship:

The Taguchi methodology is a potent extra resource for creating high-quality methods. This unified approach is easy to understand and use, and it yields optimal design, implementation, quality, and cost.

International Journal For Advanced Research In Science & Technology
A peer reviewed international journal www.ijarst.in
ISSN: 2457-0362

Step 1: Taguchi Method

The larger, the better for the S/N ratio $-10\log_{10}\frac{1}{n}\sum_{i=1}^{n}\frac{1}{y_i^2}$

The smaller, the better for the S/N ratio $-10\log_{10}\frac{1}{n}\sum_{i=1}^{n}y_i^2$

Step 2:Normalization of S/N ratios between 0 and 1 using Eq. 3 and Eq. 4.

k = 1 ton, I = 1 to 18, where n is the performance attribute, and I is the experimental number. x(∗(k)is the significance subsequently grey relational generation, the minimum is x(∗(k), which is the lowest value of x(∗(k), and max x(“(k) is the highest value of x(“(k).

This is the larger, the better:

Table 6. Taguchi Analysis: GRG versus T, N, and F of S/N ratios and means.

$$x_i^*(k)=\frac{x_i^0(k)-\min x_i^0(k)}{\max x_i^0(k)-\min x_i^0(k)}$$

This is the smaller, the better:

$$x_i^*(k)=\frac{\max x_i^0(k)-x_i^0(k)}{\max x_i^0(k)-\min x_i^0(k)}$$

Step 3:To evaluate the grey relational coefficient (GRC)using Equation 5.

The grey relation coefficient $\xi_i(k)$ can be determined as follows:

$$\xi_i(k)=\frac{\Delta_{min}+\zeta\Delta_{max}}{\Delta_{oi}(k)+\zeta\Delta_{max}}$$

Step 4: To calculate the grey relational grade (GRG) by using Equation 6:

$$\frac{1}{n}\sum_{i=1}^{n}\xi_i(k)=\gamma_i$$

Step: 5: The purpose of this analysis of variance (ANOVA) is to determine the best value for the GRG parameter that may be achieved by adjusting the values of the other process parameters. Surface roughness, uniaxial tensile strength, and microhardness are investigated as a function of three input parameters: weld process conditions, TRS, and TTS. Table 4 displays Taguchi's L18 OA.

Table 3. FSW process parameters are arranged in a tabular form.

Parameter designation	Process parameter	LEVELS		
		Level 1	Level2	Level3
T	Type of Welding Process-T	NFSW	SFSW	****
N	Tool Rotational Speed (rpm)-N	1100	1250	1400
F	Tool Transverse speed(mm/min)-F	22	45	60

RESULTS AND DISCUSSION

The combined responses identified using GRA may reveal the impact of process factors in advance. The S/N ratio based on the Taguchi method is used to solve the GRG and determine the ranking in the GRA. Using Eq. [5], we calculate all of the GRC significances for a total of 18 trials. Use of Eq. [6] allows regulation of GRGs for all operation characteristics.

Table 4. Test results and S/N ratios data

Expt No	Process parameters			Test Results			S/N ratios		
	T	N	F	UTS(Mpa)	Ra(μm)	HV	UTS	Ra	HV
1	SFSW	1100	22	154.85	0.84	94	43.798	1.514	39.463
2	SFSW	1100	45	148.78	0.91	91	43.451	0.819	39.181
3	SFSW	1100	60	146	0.96	88	43.287	0.355	38.89
4	SFSW	1250	22	167.41	0.76	98	44.476	2.384	39.825
5	SFSW	1250	45	157.73	0.81	96	43.958	1.83	39.645
6	SFSW	1250	60	155.99	0.86	94	43.862	1.31	39.463
7	SFSW	1400	22	175.63	0.57	109	44.892	4.883	40.749
8	SFSW	1400	45	165.32	0.66	103	44.367	3.609	40.257
9	SFSW	1400	60	160.06	0.75	96	44.086	2.499	39.645
10	NFSW	1100	22	150.95	0.92	92	43.577	0.724	39.276
11	NFSW	1100	45	143.35	0.97	88	43.128	0.265	38.89
12	NFSW	1100	60	136.58	0.98	85	42.708	0.175	38.588
13	NFSW	1250	22	163.33	0.72	93	44.261	2.853	39.37
14	NFSW	1250	45	153.49	0.82	91	43.722	1.724	39.181
15	NFSW	1250	60	147.04	0.96	89	43.349	0.355	38.988
16	NFSW	1400	22	168.16	0.64	103	44.514	3.876	40.257
17	NFSW	1400	45	158.35	0.78	98	43.992	2.158	39.825
18	NFSW	1400	60	154.05	0.8	94	43.753	1.938	39.463

Ra, HV, and UTS have a 0.2, 0.3, and 0.5 weightage in operational properties, respectively [Kundu et al.]; this is supported by data indicating the output parameter's importance in practice. In Table 5 we can see the computed GRC and GRG for each experiment. Table 5 shows that experiment 7 has a higher GRG value, which indicates that better-quality features were produced on the larger GRG; the optimal amount of every controllable factor was maintained.

International Journal For Advanced Research In Science & Technology
A peer reviewed international journal www.ijarst.in
ISSN: 2457-0362

table 5. Normalization, Deviation Sequence, GRC, and GRG Data.

Expt NO	Normalization			Deviation sequence			GRC			GRG	Rank
	UTS	Ra	HV	UTS	Ra	HV	UTS	Ra	HV		
1	0.499	0.716	0.405	0.501	0.284	0.595	0.500	0.637	0.457	0.171	11
2	0.340	0.863	0.274	0.660	0.137	0.726	0.431	0.785	0.408	0.165	15
3	0.265	0.962	0.140	0.735	0.038	0.860	0.405	0.929	0.368	0.166	13
4	0.810	0.531	0.572	0.190	0.469	0.428	0.724	0.516	0.539	0.209	3
5	0.572	0.648	0.489	0.428	0.352	0.511	0.539	0.587	0.495	0.178	8
6	0.528	0.759	0.405	0.472	0.241	0.595	0.515	0.675	0.457	0.176	9
7	1.000	0.000	1.000	0.000	1.000	0.000	1.000	0.333	1.000	0.289	1
8	0.760	0.271	0.772	0.240	0.729	0.228	0.675	0.407	0.687	0.208	4
9	0.631	0.506	0.489	0.369	0.494	0.511	0.575	0.503	0.495	0.179	7
10	0.398	0.883	0.318	0.602	0.117	0.682	0.454	0.811	0.423	0.172	10
11	0.192	0.981	0.140	0.808	0.019	0.860	0.382	0.963	0.368	0.165	16
12	0.000	1.000	0.000	1.000	0.000	1.000	0.333	1.000	0.333	0.156	18
13	0.711	0.431	0.362	0.289	0.569	0.638	0.634	0.468	0.439	0.181	6
14	0.464	0.671	0.274	0.536	0.329	0.726	0.483	0.603	0.408	0.161	17
15	0.293	0.962	0.185	0.707	0.038	0.815	0.414	0.929	0.380	0.169	12
16	0.827	0.214	0.772	0.173	0.786	0.228	0.743	0.389	0.687	0.218	2
17	0.588	0.579	0.572	0.412	0.421	0.428	0.548	0.543	0.539	0.181	5
18	0.478	0.626	0.405	0.522	0.374	0.595	0.489	0.572	0.457	0.165	14

The mean GRG and the optimum levels of the elements are presented in Table 6. The optimum levels of the process parameters founded on the GRG are T2N3F1. It is the optimum level of the process parameter at submerged FSW, higher TRS 1400 rpm, and low TTS 22 mm/min. Fig. 5 shows a clear view of the process parameters and depicts the TRS increases, TTS decreases and submerged FSW conditions get high GRG value. The optimum process condition of the higher TRS, low tool feed rate, and Submerged FSW reveals that there is no defect due to sufficient heat generation between tool and workpiece, and it contains more refined grains in the weld zone.

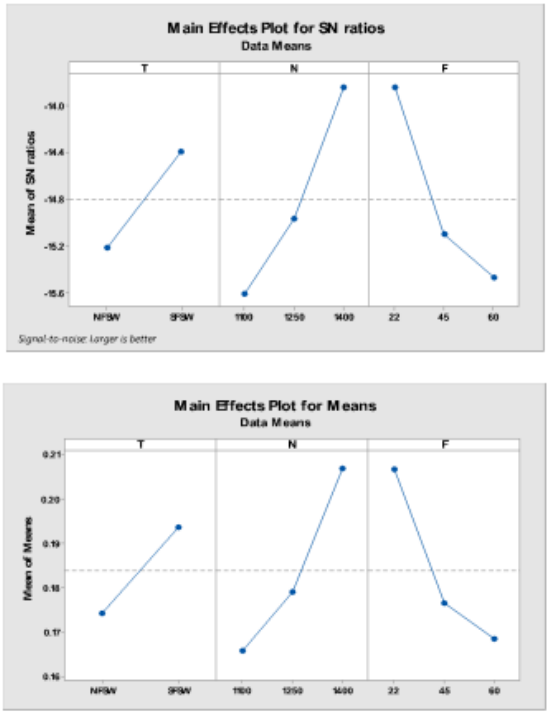

Figure 5. Response graphs of S/N ratio and mean of GRG.

The ANOVA for GRG is calculated and presented in Table 7. They were being carried away to analyze the consequences of the process parameter. The higher F-value specifies that the factor is well significant in affecting all the responses of the weld. The increased effect of the process parameters is defined as orderly TRS as 8.53, TTS as 7.69, and the type of weld nature is of the minor effect 5.33. The P-Values of all the process parameters are shown below as 0.05. This means that the process parameters are the most significant factors. % Of the contribution is at the process parameter TRS as 34.28, TTS as 30.91, the type of weld nature is 10.69, and the error in this process parameter is 24.1 at DOF 12. Finally, experimentation's total degree of freedom is 17. The predicted value is calculated based on the literature [2].

Table 6. Taguchi Analysis: GRG versus T, N, and F of S/N ratios and means.

International Journal For Advanced Research In Science & Technology
A peer reviewed international journal www.ijarst.in
ISSN: 2457-0362

Response Table for S/N RatiosLarger is better-GRG				Response Table for Means		
Level	T	N	F	T	N	F
1	-15.21	-15.61	-13.84	0.1743	0.1658	0.2067
2	-14.39	-14.96	-15.10	0.1936	0.1792	0.1766
3		-13.84	-15.47		0.2069	0.1686
Delta	0.82	1.78	1.63	0.0193	0.0411	0.0382
Rank	3	1	2	3	1	2

Table 7. The ANOVA of GRG of UTS, Ra, and HV.

Source	DF	Adj SS	Adj MS	F-Value	P-Value	% of contribution
T	1	3.021	3.0208	5.33	0.040	10.69
N	2	9.680	4.8401	8.53	0.005	34.28
F	2	8.729	4.3644	7.69	0.007	30.91
Error	12	6.806	0.5672			24.10
'Total	17	28.236				

Predicted value of GRG= $T_2+N_3+F_1-2T_{mean}$

$= 0.1936+0.2069+ 0.2067-2*0.1729$

$=0.2614$

The actual GRG optimum value is 0.289, and the predicted value is 0.2614. The error is 0.0276, and then the percentage of error is 9.55.

Fracture Analysis:

The fracture performance of FSW specimens is being studied, and the fracture UTS specimens are being investigated. SEM is used to analyse the fracture surfaces' microstructural topographies. Figure 6 (a) and (b) show scanning electron microscopy images of reference specimens (b). The dimpled structure seen on the surface of the fracture specimen is indicative of ductile failure. Numerous distorted dimples before to collapse indicate plastic deformation. The Normal FSW fracture surface is covered with many little dimples.

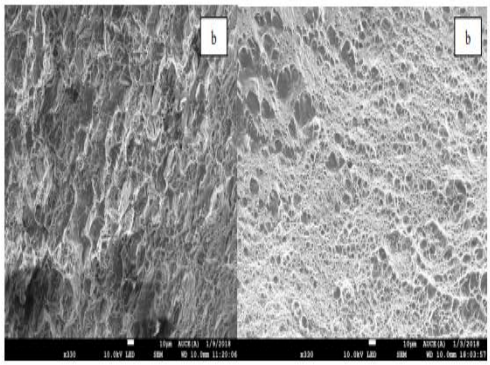

Figure 6. SEM images. a) Submerged FSW, 1400 rpm, 22 mm/min. b) Normal FSW 1400 rpm, 22mm/min.

The fracture specimens of the weld joints perform ductile features using a method to control dimples, but the dimples on the fracture surface of the joints welded in air (Fig. 6a) look smaller and more evenly distributed than the dimples on the fracture surface of the joints welded in water (Fig. 6b). Consistent with the findings, they indicate a high UTS. Higher densities of tiny grains everywhere around the optimal region were found in a scanning electron microscopy investigation.

The center welds line is a specification for maximum durability. The tensile specimen cracks at an angle of 45 degrees, retreating side up. The EDS analysis in Fig.7 reveals the optimal welding techniques' chemical make-up.

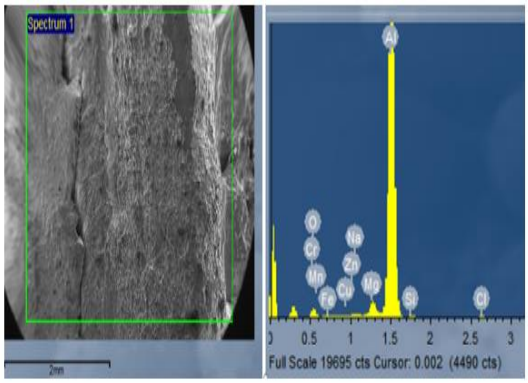

Figure 7. EDS for optimum process parameters Submerged FSW, 1400 rpm, 22 mm/min.

CONCLUSION

The Taguchi technique was used here to determine each respondent's share (in percentage terms) of the final result. Using ANOVA, the relative importance of each process parameter is determined. Multi-

objective process parameters for FSW AA5083 have been optimized by Taguchi-based GRA. The findings presented here are based on this inquiry. First, a TRS speed of 1400 rpm, a TTS speed of 22 mm/min, and a submerged FSW process will provide the highest UTS, the lowest microhardness, and the smoothest surface roughness of the FSW weld bead, respectively. The percentage-based ANOVA of UTS, Ra, and HV GRG is analysed. 10.69%, 34.28%, and 30.91% are the TRS, TTS, and weld condition percentages. Therefore, by adjusting parameters in the order of increased TRS, submerged FSW, and reduced TTS, we may get excellent welds with increased strength and hardness. Fourth, the Submerged FSW sample showed tensile strength that was closer to the strength of the underlying material. This means that even under fully immersed FSW circumstances, enough heat is created to maintain life. 5. The tensile test specimen is broken to the retreating side with 450 degrees of inclination, and the SEM examination of the optimum level fractured specimen reveals that increased density of the tiny grains specifies better strength.

REFERENCES

[1] Sree Sabari, S., et al. 2016. Experimental and Numerical Investigation on Under-Water Friction Stir Welding of Armour Grade AA2519-T87 Aluminium Alloy. Defence Technology, vol. 12, no. 4, Elsevier B.V., 2016, pp. 324–33, doi:10.1016/j.dt.2016.02.003.

[2] Sabari, S. Sree, et al. 2016. Influences of Tool Traverse Speed on Tensile Properties of Air Cooled and Water Cooled Friction Stir Welded AA2519-T87 Aluminium Alloy Joints. Journal of Materials Processing Technology, vol. 237, Elsevier B.V., 2016, pp. 286–300, doi: 10.1016/j.jmatprotec.2016.06.015.

[3] Fuji, H.; Cui, L.; Maeda, M.; Nagi, K. 2006. Effect of tool shape on mechanical properties and microstructure of friction stir welded aluminium alloys. Materials Science and Engineering A 2006, 419, 25–31.

[4] Suresh, C. N., et al. 2011. A Study of the Effect of Tool Pin Profiles on Tensile Strength of Welded Joints Produced Using Friction Stir Welding Process. Materials and Manufacturing Processes, vol. 26, no. 9, 2011, pp. 1111–16, doi:10.1080/10426914.2010.532527. Darras B and Kisha E. 2013.

[5] Submerged friction stir processing of AZ31 magnesium alloy. Mater Design 2013; 47: 133–137 Hofmann D and Vecchio K. 2005. Submerged friction stirs pro- cessing (SFSP): an improved method for creating ultra- fine-grained bulk materials. Mater Sci Eng. A 2005; 402: 234–241.

[6] S. Shanaaz, J. Edwin Raja Dhaks, and N. Murunga. 2018. Weldability of marine grade AA 5052 aluminium alloy by underwater friction stir welding, Int. J. Adv. Manuf. Technol., vol. 95, no. 9–12, pp. 4535–4546, doi:10.1007/s00170-017-1492-6.

[7]Pitapat, S. R., Param guru, D., & Awang, M. (2017). Microhardness and Microstructural Studies on Submerged Friction Stir Welding of 5052 Aluminium Alloy. Volume 2: Advanced manufacturing.doi:10.1115/imece2017-71248.

[8] Jata, K.V.; Semiatin, S.L. 2000. Continuous dynamic recrystallization during friction stir welding of high strength aluminum alloys. Scripta Materialia 2000, 43, 743. Liu, G.; Murr, L.E.; Niou, C.S.; McClure, J.C.; Vega, F.R. 1997.

[9] Micro structural aspects of the friction stir welding of 6061-T6 aluminum. Scripta Materialia, 37, 355.

[10] M. Koilraj a, V. Sundareswaran b, S. Vijayan c, S.R. Koteswara Rao d. 2012. Friction stir welding of dissimilar aluminum alloys AA2219 to AA5083 – Optimization of process parameters using Taguchi technique Materials and Design 42 (2012) 1–7 doi: 10.1016/j.matdes.2012.02.016.

[11] Khalkhal, Abolfazl, MurtazaSarmad, and Ehsan Sarukhan. 2017. Investigation on the Best Process Criteria for Lap Joint Friction Stir Welding of AA1100 Aluminium Alloy via Taguchi Technique and ANOVA, Proceedings of the Institution of Mechanical Engineers, Part E: Journal of Process Mechanical Engineering, 231.2,329–42. https://doi.org/10.1177/0954408916665651.

[12] Taguchi G and Kenisha S. Orthogonal arrays and linear graphs, tools for quality engineering. MI, USA: American Supplier Institute (ASI), 1987, 72 pp.

[13] Taguchi G. 1986. Introduction to quality engineering. New York: Kraus International Publication. J. Deng. 1989. Introduction to the grey system. J Grey Systems, 1 – 24.

[14] Dinesh Kumar, R., M. S. Ilhar Ul Hassan, S. Muthu Kumaran, T. Venkateshwara, and D. Sivakumar. 2019. Single and Multi-Response Optimization and Validation of Mechanical

Properties in Dissimilar Friction Stir Welded AA2219-T87 and AA7075-T73 Alloys Using T-GRA, Experimental Techniques, 43.3 (2019), 245–59, https://doi.org/10.1007/s40799-019-00305-3.